

# Dust Properties in the FUV in Ophiuchus

N. V. Sujatha, P. Shalima, Jayant Murthy

sujaskm@yahoo.co.in, shalima.p@gmail.com, jmurthy@yahoo.com

*Indian Institute of Astrophysics, Koramangala, Bangalore - 560 034, India*

and

Richard Conn Henry

henry@jhu.edu

*Department of Physics and Astronomy, The Johns Hopkins University,  
Baltimore, MD 21218*

## ABSTRACT

We have derived the albedo ( $a$ ) and phase function asymmetry factor ( $g$ ) of interstellar dust grains at  $1100 \text{ \AA}$  using archival *Voyager* observations of diffuse radiation in Ophiuchus. We have found that the grains are highly forward scattering with  $g = 0.55 \pm 0.25$  and  $a = 0.40 \pm 0.10$ . Even though most of the gas in this direction is in the Ophiuchus molecular cloud, the diffuse FUV radiation is almost entirely due to scattering in a relatively thin foreground cloud. This suggests that one cannot assume that the UV background is directly correlated with the total amount of gas in any direction.

*Subject headings:* dust – ultraviolet: ISM – infrared: ISM

## 1. INTRODUCTION

The Ophiuchus molecular cloud is one of a large complex of clouds at a distance of about 160 pc from the Sun (Chen et al. 1997). The region has been extensively studied in CO (de Geus et al. 1990; Dame et al. 2001) as well as with four-colour photometry (Corradi et al. 2004) allowing us to determine the three-dimensional distribution of the matter in this direction. Our

interest in this region is that one of the first observations of diffuse emission in the far ultraviolet (FUV – 912 - 1216  $\text{\AA}$ ) was made here by Holberg (1990) who identified the emission as starlight from the nearby Scorpius-Centaurus OB association scattered by dust in the Ophiuchus molecular cloud.

Because of the technical difficulties inherent in diffuse observations in the FUV, largely due to scattering from the intense

geocoronal Ly $\alpha$  line, there have been very few observations of the background radiation in this spectral region (see Bowyer 1991; Henry 1991, for reviews of the diffuse radiation in both the near and far ultraviolet). By far the largest and most reliable data set has come from the ultraviolet spectrographs (UVS) aboard the two Voyager spacecraft which made observations of various astrophysical targets during the interplanetary phase of their mission, between their hugely successful planetary encounters. Many of these targets were of objects with no intrinsic FUV flux and Murthy et al. (1999) used them for a comprehensive study of the diffuse FUV radiation field. Because of the sensitivity of the Voyager UVS to diffuse radiation and the distance of the spacecraft far from the Earth where emission from interplanetary H I is minimized, these remain the definitive observations of the diffuse radiation field in the FUV.

Except for a small extragalactic component at high latitudes (Henry 1991), the diffuse UV radiation is largely due to starlight scattered by interstellar dust and as such can be used to derive the scattering properties of the interstellar dust grains. Unfortunately there has been considerable controversy about both the level of the diffuse radiation and the modeling used to extract the optical constants (see Draine 2003a; Mathis et al. 2002, for a discussion of the difficulties) and there have been only loose observational constraints on the albedo ( $a$ ) and phase function asymmetry factor ( $g$ ) of the dust grains.

As mentioned above, Holberg (1990) discovered intense diffuse emission from Ophiuchus using the Voyager UVS and in-

terpreted this emission as starlight back-scattered by the Ophiuchus molecular cloud. We have reexamined these observations along with others from the Voyager archives (Murthy et al. 1999) in the light of a more sophisticated model and an improved understanding of the dust distribution in the direction of Ophiuchus (Corradi et al. 2004) and have found that the emission is actually due to the forward scattering of the light from a much lower density sheet of material in front of the Ophiuchus molecular cloud. There were many observations spread throughout the entire region and so we have been able, for the first time, to remove the degeneracy between the albedo ( $a$ ) and the phase function asymmetry parameter ( $g$ ) which have plagued studies of the diffuse radiation (Draine 2003a). We have constrained  $a$  to  $0.40 \pm 0.10$  and  $g$  to  $0.55 \pm 0.25$ , in good agreement with the theoretical prediction of Weingartner & Draine (2001) for a mixture of graphitic and silicate grains.

## 2. OBSERVATIONS

The two Voyager spacecraft include identical Wadsworth-mounted objective grating ultraviolet spectrographs (UVS) covering the wavelength region between 500 and 1700 Å, with their greatest sensitivity at wavelengths below 1200 Å. The field of view of the spectrographs is  $0.1^\circ \times 0.87^\circ$  with a spectral resolution of 38 Å for diffuse sources. The spacecraft were launched within two weeks of each other — Voyager 2 in 1977 August and Voyager 1 in 1977 September — and obtained a wealth of information on all four of the giant planets. The two spacecraft are still continuing operation at the edge

of the solar system with more than 10,000 days of operation each. A full description of the UVS spectrographs and further information about the interstellar mission of the Voyager spacecraft is given by Holberg & Watkins (1992).

While the spacecraft were between planetary encounters, they observed many astronomical targets. Amongst these targets were a series of scans in the vicinity of Ophiuchus with the Voyager 2 spacecraft in 1982 (Holberg 1990). We have supplemented these with further observations from the Voyager archives taken at various times between 1982 and 1994 (Murthy et al. 1999). There were a total of 31 such locations and these are plotted on an IRAS 100  $\mu\text{m}$  map in Fig. 1 and tabulated in Table 1 with the total hydrogen column density (Schlegel et al. 1998) and the IRAS 100  $\mu\text{m}$  flux (Wheelock et al. 1994). There was a limit cycle motion of a few tenths of a degree in the Voyager pointing and the position reported in the table is an average of the actual pointing of the instrument.

The data used here are from Murthy et al. (1999) and are available from the authors. The data reduction is fully described in that paper and in Holberg (1986) and consists of fitting three components to the observed signal: dark noise from the spacecraft’s radioisotope thermoelectric generator (RTG); emission lines from interplanetary H I; and emission from cosmic sources. The dark noise was subtracted using the continuum below the Lyman limit 912  $\text{\AA}$  and the astronomical and heliospheric emission were then simultaneously fit using templates for the emission. This reduction procedure was shown to be consistent and reproducible over observa-

tions separated widely in time and between the two spacecraft and yielded  $1\sigma$  limits as low as 30 photons  $\text{cm}^{-2} \text{s}^{-1} \text{sr}^{-1} \text{\AA}^{-1}$  over a large part of the sky. For the bright sources reported on here, the diffuse emission dominated the raw data and there was little uncertainty in the derived levels.

### 3. MODEL

The diffuse emission in Ophiuchus is the result of light from the nearby stars scattering from interstellar dust in the line of sight and were modeled in a similar manner to Shalima & Murthy (2004) in the Coal-sack. The stellar radiation field was calculated at the location of the scattering dust using the model of Sujatha et al. (2004), in which the distance and spectral type of each star was taken from Hipparcos data (Perryman et al. 1997) and the flux calculated using Kurucz models (Kurucz 1992) with the latest modifications from his web page (<http://kurucz.harvard.edu>). Eight stars (see Fig. 1) contribute  $\sim 90\%$  of the total ISRF in this region. The properties of the stars are given in Table 2.

The amount of radiation scattered to the observer is dependent on the scattering function of the grains and we have used the Henyey-Greenstein scattering phase function,  $\phi(\theta)$  (Henyey & Greenstein 1941).

$$\phi(\theta) = \frac{a}{4\pi} \frac{(1 - g^2)}{(1 + g^2 - 2g\cos(\theta))^{1.5}} \quad (1)$$

Here  $a$  is the albedo — which can range from 0 for dark grains to 1 for fully reflecting grains — and  $g$  is the phase function asymmetry factor with  $g = 0$  indicating isotropic scattering and higher values indicating forward scattering grains.

Draine (2003b) has suggested that the Henyey-Greenstein function underestimates the scattered radiation for highly forward scattering grains ( $g > 0.7$ ) in the FUV. We have found, empirically, that using the theoretical scattering function of Weingartner & Draine (2001) for a mixture of graphite and silicate grains makes no more than a 10% difference in the derivation of the optical constants for  $g = 0.65$  and so, for consistency with the literature, we only cite the results using the Henyey-Greenstein function. The primary uncertainty in our procedure is in the location of the scattering dust and we discuss this below.

The interstellar medium in the direction of Ophiuchus is dominated by the huge molecular complexes in Ophiuchus (Fig. 1) at a distance of  $\sim 160$  pc (Chen et al. 1997). Because of the thickness of the cloud, only foreground stars will contribute to the diffuse radiation observed at the Earth. Back-scattering from the molecular cloud is an order of magnitude too small to account for the observed UV intensity and hence we conclude that the scattering must be from two extended sheet-like structures which Corradi et al. (2004) have shown to cover the entire region between the galactic longitudes of  $290^\circ - 10^\circ$  and latitudes of  $-25^\circ - +25^\circ$ . The nearer of the two sheets is at a distance of  $d \leq 60$  pc from the Sun and the other, from which most of our observed scattering comes, lies between 100 and 150 pc from the Sun, depending on the direction. The latter sheet is likely part of the neutral ring surrounding the complex of molecular clouds in Ophiuchus discovered by Egger & Aschenbach (1995) in the ROSAT all-sky survey. Corradi et al. (2004) has found a column density of  $3.2$

$\times 10^{19}$   $\text{cm}^{-2}$  in the nearer cloud and a much larger column density of  $3.7 - 27 \times 10^{20}$   $\text{cm}^{-2}$  in the further cloud. Other than these two clouds and the Ophiuchus molecular cloud, there is very little material out to a distance of at least 200 pc from the Sun (Frisch et al. 2005).

In our model, we have divided the total H I from Dickey & Lockman (1990) in any line of sight into the two foreground clouds, with a constant value of  $3.2 \times 10^{19}$   $\text{cm}^{-2}$  in the nearer cloud and the rest in the further cloud. For the Ophiuchus molecular clouds, we have subtracted the H I column density from the total hydrogen column density of Schlegel et al. (1998) and distributed this excess material at the location of the molecular cloud. We converted the H I column density to a dust scattering cross-section using the theoretical values of Weingartner & Draine (2001), implicit in which is the dust to gas ratio of Bohlin et al. (1978). In practice, the observed UV emission is almost entirely from the more distant of the two sheets and so is most sensitive to the exact distance of that sheet, or rather to the distance between the sheet and the stars dominating the ISRF in this region, and the amount of dust in that cloud. Because this distance is uncertain, we have used a 3 parameter model in which we allow the distance to the dust to vary but fix  $a$  and  $g$  to a common value over all 31 positions. We then use a single scattering model to calculate the scattered flux in the UV and independently calculate the thermal emission at  $100 \mu\text{m}$  for the best fit parameters. The best fit distances are plotted in Fig. 2 and show a variation of 100 - 125 pc in this region, consistent with the values found by Corradi et al. (2004).

## 4. RESULTS AND DISCUSSION

It is interesting to note that the level of the diffuse emission is not at all correlated with the amount of material in the line of sight (Fig. 3). Instead there is a tight correlation between the level of the ISRF and the scattered radiation (Fig. 4). This has important implications for the study of the diffuse radiation field. It is often claimed that the diffuse radiation is correlated with the H I column density (e.g. Bowyer 1991; Schiminovich et al. 2001); however, it is becoming increasingly evident that the diffuse radiation is dominated by local effects, particularly near bright stars (c.f. Murthy & Sahnou 2004).

Our model predictions match the observations extremely well both in UV scattering (Fig. 5) and in 100  $\mu\text{m}$  infrared emission (Fig. 6). We have derived a 90% confidence contour (as per Lampton, Margon, & Bowyer 1976) for  $a$  and  $g$  and this is shown in Fig. 7. Our 90% confidence limits on  $a$  and  $g$  are  $0.40 \pm 0.10$  and  $0.55 \pm 0.25$  respectively and are consistent with the theoretical predictions of Weingartner & Draine (2001) for average Milky Way dust with  $R_V=3.1$ .

There are very few determinations of the optical parameters of interstellar grains at wavelengths shorter than 1200  $\text{\AA}$  (Draine 2003a; Gordon 2004) and most of these have come from observations of reflection nebulae. Witt et al. (1993) found an albedo of  $0.42 \pm 0.04$  from *Voyager 2* observations of NGC 7023 and Burgh et al. (2002) found an albedo of  $0.30 \pm 0.10$  from rocket observations of NGC 2023. Both groups claimed that the grains were highly forward scattering with  $g \sim 0.8$ . Shalima

& Murthy (2004) found a similar value of  $0.40 \pm 0.20$  through *Voyager* observations of the Coalsack Nebula but were not able to constrain  $g$ .

Although our derived albedo ( $0.40 \pm 0.10$ ) is consistent with the earlier determinations, we find a slightly lower value for  $g$  ( $0.55 \pm 0.25$ ). It is possible that conditions are different in reflection nebulae as opposed to the diffuse ISM we observe or it may be that, as Draine (2003b) suggests, the scattering function is poorly represented by the Henyey-Greenstein function in the FUV leading to differences between determinations in different geometries, particularly for highly forward scattering grains.

## 5. CONCLUSIONS

We have used *Voyager* observations of the diffuse FUV radiation in the region of Ophiuchus to investigate the optical constants of the interstellar dust grains. We have found that the intense emission in this region arises not in the dense molecular cloud which contains most of the matter in this direction but rather in a much thinner neutral sheet in front of the cloud. In fact, there is no correlation between either the 100  $\mu\text{m}$  IRAS emission or  $N(\text{H})$  and the scattered FUV light. Instead the FUV emission is tightly correlated with the strength of the local ISRF. Thus unlike thermal dust emission in the IR, where the dust is optically thin and the material along the entire line of sight contributes to the total, scattering in the FUV requires much thinner clouds and nearby bright stars.

In general, one should not expect correlations on global scales between the UV

and IR or UV and N(H). This is borne out by Murthy & Sahnow (2004) who find only a mild dependence on the 100  $\mu\text{m}$  for the FUV flux but not by Schiminovich et al. (2001) who claim a correlation between the UV (at 1500  $\text{\AA}$ ) and N(H) using data from the NUVIEWS rocket flight. We are pursuing further investigations with data from the Galaxy Evolution Explorer (GALEX) to test these correlations.

We find that the interstellar dust grains are highly forward scattering with a  $g$  ( $= \langle \cos\theta \rangle$ ) of  $0.55 \pm 0.25$  and an albedo of  $0.40 \pm 0.10$ . These results are in general agreement both with the theoretical predictions of Weingartner & Draine (2001) and previous observations of reflection nebulae. As a test of our model, we have independently calculated the 100  $\mu\text{m}$  intensities for each of the locations for our best fit  $a$  and  $g$  values and found them to match the IRAS (100  $\mu\text{m}$ ) observations.

We thank an anonymous referee for useful comments which helped to clarify parts of the paper. We acknowledge the use of NASA's *SkyView* facility (<http://skyview.gsfc.nasa.gov>) located at NASA Goddard Space Flight Center. NVS is supported by a RESPOND grant from the Indian Space Research Organization (ISRO). PS and JM are supported by the Indian Institute of Astrophysics (IIA), an autonomous institution funded by the Department of Science and Technology (DST). RCH is supported by Maryland Space Grant Consortium.

## REFERENCES

- Bohlin, R. C., Savage, B. D., & Drake, J. F. 1978, *ApJ*, 224, 132
- Bowyer, S. 1991, *ARA&A*, 29, 59
- Burgh, E. B., McCandliss, S. R., & Feldman, P. D. 2002, *ApJ*, 575, 240
- Chen, H., Grenfell, T. G., Myers, P. C., & Hughes, J. D. 1997, *ApJ*, 478, 295
- Corradi, W. J. B., Franco, G. A. P., & Knude, J. 2004, *MNRAS*, 347, 1065
- Dame, T. M., Hartmann, D., & Thaddeus, P. 2001, *ApJ*, 547, 792
- de Geus, E. J., Bronfman, L., & Thaddeus, P. 1990, *A&A*, 231, 137
- Dickey, J. M., & Lockman, F. J. 1990, *ARA&A*, 28, 215
- Draine, B. T. 2003a, *ARA&A*, 41, 241
- . 2003b, *ApJ*, 598, 1017
- Egger, R. J., & Aschenbach, B. 1995, *A&A*, 294, L25
- Frisch, P. C., Müller, H. R., Zank, G. P., & Lopate, C. 2005, In *Astrophysics of Life*, Proc. of STScI Symp., 2002, Vol. 16, ed. M. Livio, I. N. Reid & W. B. Sparks (UK: Cambridge University Press), 21
- Gordon, K. D. 2004, in *ASP Conf. Series*, 309, *Astrophysics of Dust*, ed. A. N. Witt, G. C. Clayton & B. T. Draine (San Francisco: ASP), 77
- Henry, R. C. 1991, *ARA&A*, 29, 89
- Henyey, L. C., & Greenstein, J. L. 1941, *ApJ*, 93, 70

- Holberg, J. B. 1986, *ApJ*, 311, 969
- . 1990, in *The Galactic and Extragalactic Background Radiation*, IAU Symp., 139, ed. S. Bowyer & C. Leinert (Dordrecht: Kluwer), 220
- Holberg, J. B., & Watkins, R. 1992, *Voyager Ultraviolet Spectrometer Guest Observer and Data Analysis Handbook*, Version 1.1, unpublished
- Kurucz, R. L. 1992, in *The Stellar Populations of Galaxies*, IAU Symp., 149, ed. B. Barbuy & A. Renzini (Dordrecht: Kluwer), 225
- Lampton, M., Margon, B., & Bowyer, S. 1976, *ApJ*, 208, 177
- Mathis, J. S., Whitney, B. A., & Wood, K. 2002, *ApJ*, 574, 812
- Murthy, J., Hall, D., Earl, M., Henry, R. C., & Holberg, J. B. 1999, *ApJ*, 522, 904
- Murthy, J., & Sahnou, D. J. 2004, *ApJ*, 615, 315
- Perryman, M. A. C., Lindegren, L., Kovalevsky, J., Hog, E., Bastian, U., Bernacca, P. L., Creze, M., Donati, F., Grenon, M., van Leeuwen, F., van der Marel, H., Mignard, F., Murray, C. A., Poole, R. S. L., Schrijver, H., Turon, C., Arenou, F., Froeschl, M., & Petersen, C. 1997, *A&A*, 323, 49
- Schiminovich, D., Friedman, P. G., Martin, C., & Morrissey, P. F. 2001, *ApJ*, 563, 161
- Schlegel, D. J., Finkbeiner, D. P., & Davis, M. 1998, *ApJ*, 500, 525
- Shalima, P., & Murthy, J. 2004, *MNRAS*, 352, 1319
- Sujatha, N. V., Chakraborty, P., Murthy, J., & Henry, R. C. 2004, *BASI*, 32, 151
- Weingartner, J. C., & Draine, B. T. 2001, *ApJ*, 548, 296
- Wheelock, S., Gautier III, T. N., Chillemi, J., Kester, D., McCallon, H., Oken, C., White, J., Gregorich, D., Boulanger, F., Good, J., & Chester, T. 1994, *IRAS Sky Survey Atlas Explanatory Supplement* (JPL 94-11; Pasadena: JPL)
- Witt, A. N., Petersohn, J. K., Holberg, J. B., Murthy, J., Dring, A., & Henry, R. C. 1993, *ApJ*, 410, 714

---

This 2-column preprint was prepared with the AAS L<sup>A</sup>T<sub>E</sub>X macros v5.2.

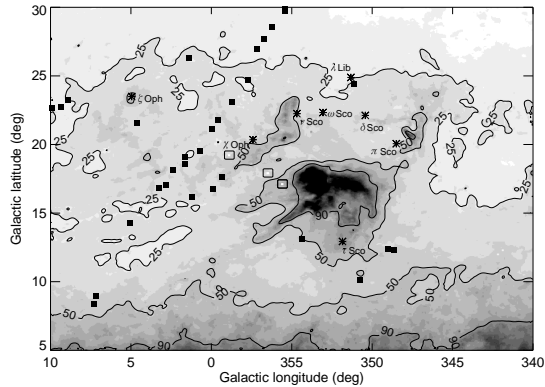


Fig. 1.— IRAS 100  $\mu\text{m}$  map of the region is shown with contours labelled in units of  $\text{MJy sr}^{-1}$ . The filled squares show the locations of the *Voyager* observations and the asterisks show the positions of the brightest UV stars in the region.

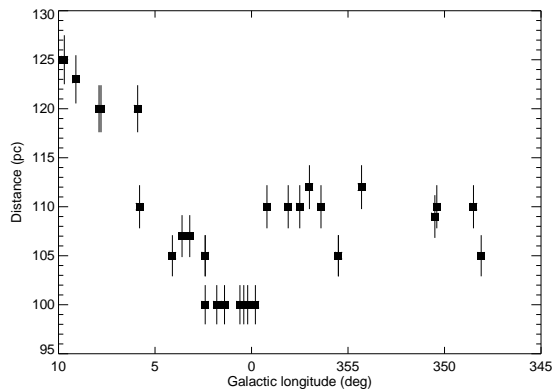


Fig. 2.— Best fit distances to the scattering layer for each of the locations as a function of galactic longitude in degrees.

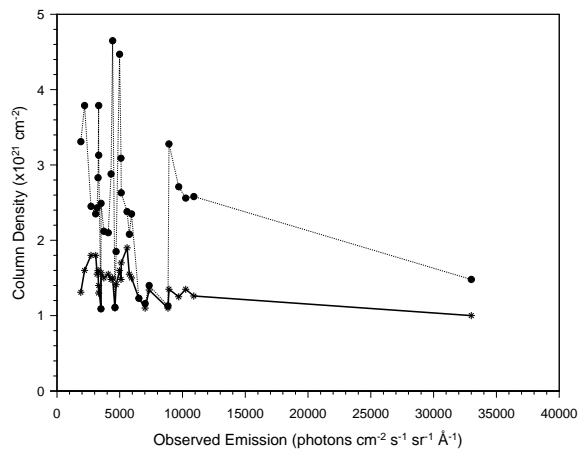


Fig. 3.— Observed UV intensity at each location is plotted against the corresponding values of the total,  $N(\text{H})$  (dotted line) and neutral,  $N(\text{H I})$  (solid line) hydrogen column densities. There is clearly no correlation between the FUV intensity and either  $N(\text{H})$  or  $N(\text{H I})$ .



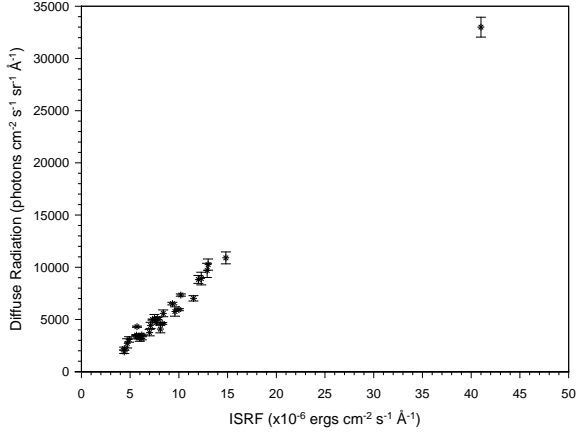


Fig. 4.— Observed UV intensity at each location is plotted against the ISRF. The non-zero intercept is due to the absorption of the diffuse radiation in the intervening ISM.

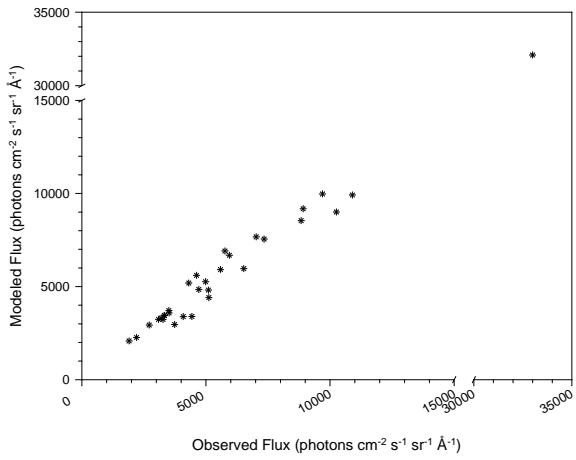


Fig. 5.— Modeled FUV ( $1100 \text{ \AA}$ ) intensities corresponding to  $a = 0.40$  and  $g = 0.6$  have been plotted against the observed values for each location.

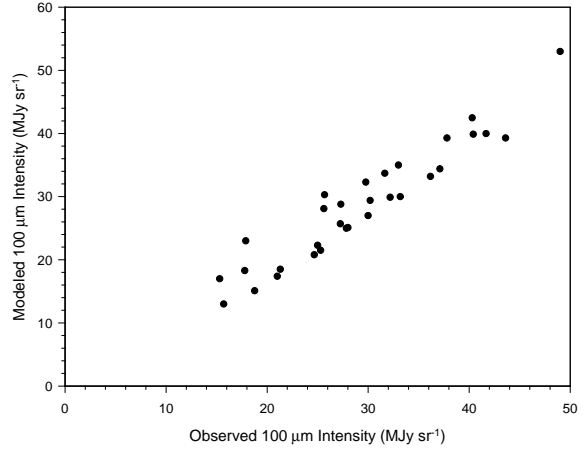


Fig. 6.— Modeled IR intensities corresponding to an albedo of 0.40 and  $g = 0.6$  have been plotted against the observed IRAS ( $100 \mu\text{m}$ ) values for each location.

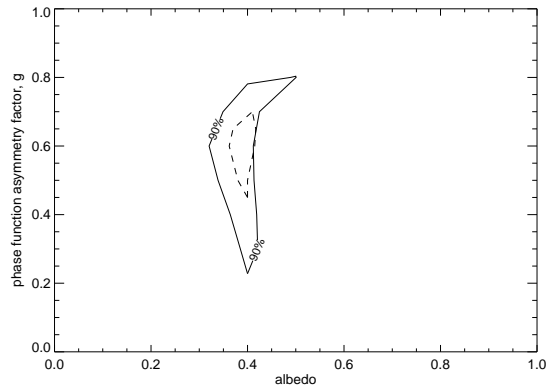


Fig. 7.— 90% confidence contour for all 31 locations (solid contour) is shown. The contour corresponds to a limit of  $0.40 \pm 0.10$  and  $0.55 \pm 0.25$  on the albedo and  $g$  respectively. Also plotted is the intersection of the individual 90% confidence contours for each of the locations (dashed line).

TABLE 1  
 DETAILS OF OBSERVED LOCATIONS IN OPHIUCHUS

Location	l (deg)	b (deg)	Observed Flux±Error (ph cm <sup>-2</sup> s <sup>-1</sup> sr <sup>-1</sup> Å <sup>-1</sup> )	IRAS(100 μm) <sup>a</sup> (MJy sr <sup>-1</sup> )	N(H) <sup>b</sup> (× 10 <sup>21</sup> cm <sup>-2</sup> )
1	359.8	17.8	1900±170	43	3.3
2	0.2	22.1	2200±140	38	3.8
3	7.9	7.8	2710±440	21	2.5
4	7.8	8.4	3090±260	17	2.4
5	0.6	21.4	3200±140	36	2.4
6	1.4	19.7	3270±360	30	2.8
7	0.4	16.8	3320±140	37	3.8
8	1.8	16.2	3320±180	32	3.1
9	355.5	31	3510±50	19	1.1
10	5.8	21.6	3510±75	33	2.5
11	2.4	19.2	3740±310	26	2.1
12	348.1	12.1	4080±360	40	2.1
13	2.4	18.7	4310±65	32	2.8
14	4.1	16.8	4430±295	30	4.7
15	355.5	30.3	4620±90	16	1.1
16	2.4	26.7	4710±150	27	1.8
17	3.6	17	4990±50	28	4.5
18	3.2	18.2	5100±90	30	3.1
19	5.9	14	5120±360	28	2.6
20	350.4	9.8	5580±325	42	2.4
21	348.5	12.2	5760±445	40	2.0
22	359.2	23.5	5940±95	33	2.4
23	357.5	27.5	6520±125	18	1.2
24	356.4	29.2	7020±260	15	1.2
25	358.1	25.2	7340±110	26	1.4
26	357	28.3	8840±380	18	1.1
27	10.2	22.4	8920±610	25	3.3
28	9.1	23.1	9700±680	27	2.7
29	9.7	22.5	10250±540	25	2.6
30	354.3	13	10900±570	49	2.6
31	350.5	24.9	33000±955	25	1.4

<sup>a</sup> Wheelock et al. (1994).

<sup>b</sup> Column densities from Schlegel et al. (1998).

TABLE 2  
 PROPERTIES OF CONTRIBUTING STARS

Star	l (deg)	b (deg)	Spectral Type	Temperature (K)	log (g)	log (z)
$\zeta$ Oph	6.28	23.59	O9V	35000	3.94	0
$\chi$ Oph	357.93	20.68	B2Vne	22000	3.94	0
$\nu$ Sco A	354.61	22.70	B2IV	22000	3.94	0
$\omega$ Sco	352.75	22.77	B1V	25600	3.94	0
$\delta$ Sco	350.10	22.49	B0.2IV	30000	3.94	0
$\pi$ Sco	347.22	20.23	B1V	25600	3.94	0
$\tau$ Sco	351.54	12.81	B0V	30000	3.94	0
$\lambda$ Lib	350.72	25.38	B3V	19000	3.94	0